

Particulate and Ammonia Concentration Measurements from a Poultry Facility in Central Iowa

FINAL REPORT

by

J. H. Prueger, W.E. Eichinger, B. Barnhardt, P. Lewandowski, R.L.
Pfeiffer and J.L. Hatfield

Sponsored by

Iowa Egg Council

IIHR Report No. _____

IIHR-Hydroscience & Engineering
College of Engineering
University of Iowa, Iowa City, IA

National Soil Tilth Laboratory, Ames, IA

December 2008

TABLE OF CONTENTS

<u>I. PROBLEM STATEMENT</u>	1
<i>Air Flow around Poultry Facilities</i>	1
<i>Objective</i>	3
<u>II. SITE DESCRIPTION</u>	3
<u>III. INSTRUMENTATION DESCRIPTION</u>	4
<i>Elastic Lidar</i>	4
<i>Ammonia Analyzer</i>	7
<i>Particle Size Analyzer</i>	8
<i>Meteorological Systems</i>	9
<u>IV. RESULTS</u>	11
<i>Particle Size Analyzer</i>	11
<i>Elastic Lidar</i>	13
<i>Ammonia Analyzer</i>	16
<i>Meteorological Systems</i>	17
<u>V. SUMMARY</u>	21
<u>VI. ACKNOWLEDGEMENTS</u>	23
<u>VII. BIBLIOGRAPHY</u>	23

LIST OF FIGURES

Figure 1. Overview of the Sparboe Pullet Facility near Eagle Grove, IA. and relative locations of the instrumentation for this study.	3
Figure 2. A photograph of the miniature elastic lidar set up to map particulates in the field. This instrument took the data in figures 1 and 2.	5
Figure 3. A photograph of the Nitrolux Ammonia analyzer. The system has a sensitivity of less than 1 ppb.	7
Figure 4. A photograph of the ELPI particle size analyzer.	8
Figure 5. Close up of EC instrumentation. Sonic anemometer and Infra-red gas analyzer.	9
Figure 6. Space between south building and windbreak. Note the 10 m EC tower near the center of the image and the multiple banks of fans	10

Figure 7. An example of the cross sectional size distribution from Aug 31. The lidar essentially measures the total of the cross sections of the particles in a given volume 11

Figure 8. The mass concentration of particulates from 31 Aug. Note the “spiked” nature of the data indicating intermittent atmospheric motions with large concentrations. 11

Figure 9. A plot of particulate concentrations derived from the lidar. This plot shows concentrations along a the length of the back of the first building (y axis) with time (x axis). Reds are highest concentrations blues are lower and white indicating ambient air. 12

Figure 10. The particulate mass concentrations from Sept. 1st. While this data seems to be less “spiked” than that from the previous day (fig 8), it isn’t. This day does contain a limited number of events with extremely high concentrations. 12

Figure 11. A plot of the lidar emission measurement concept. Measurement of the particulate concentrations upwind and downwind of the building enable estimation of the emissions from the building. 13

Figure 12. An example of a vertical slice of the atmosphere in the region between the building and windbreak. Red colors are high particulate concentrations, blues lower. White areas have ambient particulate loadings. The red area to the lower right is a north south windbreak on the far side of the building. 13

Figure 13. An example of a vertical slice of the atmosphere downwind of the first building. Three plumes are visible, one from each set of fans. Again note the amount of lofting that occurs, far above the height of the buildings. 14

Figure 14a. An example of an upwind vertical slice. The scale is changed here so that the natural variations in ambient particulate concentration can be seen. The slightly higher concentration at 400 m is from the passage of a diesel truck. The intense red at the bottom is the shape of the land surface. 15

Figure 14b. An example of a downwind vertical slice that has been inverted to obtain spatially resolved particulate mass concentrations. This plot, when combined with a wind profile will allow estimation of the particulate emission rate. 15

Figure 15. A comparison of the particulate and ammonia concentrations for Sep 1st. Note that both instruments show intermittent high concentrations at the same time. Four vertical lines are drawn to show the same times in each graph. 16

Figure 16. Variation in wind direction, speed and friction velocity for the four EC systems as a function of position in the landscape. 20

Figure 17. Depiction of the complex flow patterns developed within the channel region. uw indicates momentum or mass airflow. 21

Particulate and Ammonia Concentration Measurements from a Poultry Facility in Central Iowa

Final Report

by

J.H. Prueger, W.E. Eichinger, B. Barnhardt, P. Lewandowski, R.L. Pfeiffer and J.L. Hatfield

I. PROBLEM STATEMENT

Air Flow around Poultry Facilities

Air quality impacts of livestock production facilities have long been discussed as potential problems in rural environments (SOTF, 1995; Schiffman et al., 1995; Cunnick, 1995; Donham, 1998a; Donham, 1998b; Homes, 1995). A National Research Council (NRC) Report (2003) discussed many of the current problems and limitations in the approaches being used to quantify the emission of gases and particulates from livestock facilities and suggested that there is a lack of understanding of the dynamics of air flow. One of the conclusions reached by the NRC was the articulation of five specific short-term research needs that are required to enhance our understanding of air flow and the interactions with livestock production buildings. These recommendations included: 1) the development of protocols to determine emission rates from downwind concentration measurements; 2) the evaluation of dispersion models to determine best method to calculate fluxes; 3) the determination of best methods to establish volumetric flow rates for mechanically and naturally ventilated AFOs; 4) a comparison of emission factors for naturally and mechanically ventilated AFOs; and 5) the determination of the applicability of

utilizing PM samplers designed and calibrated for the urban environment in a rural setting (NRC, 2003). Hatfield et al. (2000) showed that air flow around earthen storage units was affected by wind direction relative to the building position and the manure storage unit demonstrating that buildings exerted a large influence on air flow patterns. There is little information on the effect of buildings on plume dispersion and, as the NRC pointed out, there needs to be further study into these dynamics.

There are observations from other systems that can guide our understanding of these dynamics. Air flow around porous versus non-porous windbreaks provide a comparison of the effects on turbulence and the wake effect of the structure. This would be analogous to naturally-ventilated buildings where air can flow through the building compared to a mechanically-ventilated building where the building acts as a bluff body where additional air movement is augmented from ventilation fans. Observations from the urban literature of air flow around houses provide an understanding of the potential effect of adjacent buildings on air flow. This is important to consider because many livestock production buildings are located adjacent to one another.

Information on plume dynamics is limited because of a lack of observation methods that can be uniformly applied to livestock buildings. The application of Light Ranging and Detection Radar (Lidar) to natural systems as a method of measuring water vapor plumes over plant canopies. Application of Lidar for water vapor has been utilized by Cooper et al. (2003) to quantify the abrupt changes in water vapor density over the riparian areas adjacent to a river. The Lidar method has been used to detect particulate movement patterns from agricultural sources (Holmen et al., 1998).

This study was designed to evaluate the turbulence (wind movement near buildings) field as measured with sonic anemometers around a mechanically ventilated poultry facility and to couple these turbulence measurements with Lidar observations of the particulate plume. Ancillary observations of 10 micron particulates and particulate size distributions provide a linkage between point measurements and spatial measurements with the Lidar.

Objective

The objective of this study was to quantify the spatial variation in the turbulence around a mechanically-ventilated poultry facility and relate these to the plume observations collected with a Lidar system.

II. SITE DESCRIPTION

The study took place at the Sparboe Pullet facility near Eagle Grove, IA during late August through mid-September of 2007. In general the facility consists of 3 large buildings with lengths oriented in an East-West direction (Figure 1). The dimensions of the buildings are approximately 180 x 16 x 12 m (600 x 54 x 40 ft) containing an average of 120,000 pullets per building. The south most building has a shelter belt comprised of three rows of trees located approximately 12 m (40 ft) from the south facing wall of the south most building. The first row of trees is Red Cedar followed by two rows of Willows. The heights of the trees were on average 5-6 m (17-20 ft). The areas between the buildings were short grass. In this study we focused primarily on the south most building (Fig. 1) measuring the turbulence or wind field in the

approach (the open area south of the wind break) between the windbreak and the south most building and the open area between the south two buildings (Fig. 1). These measurements were made in conjunction with the scanning

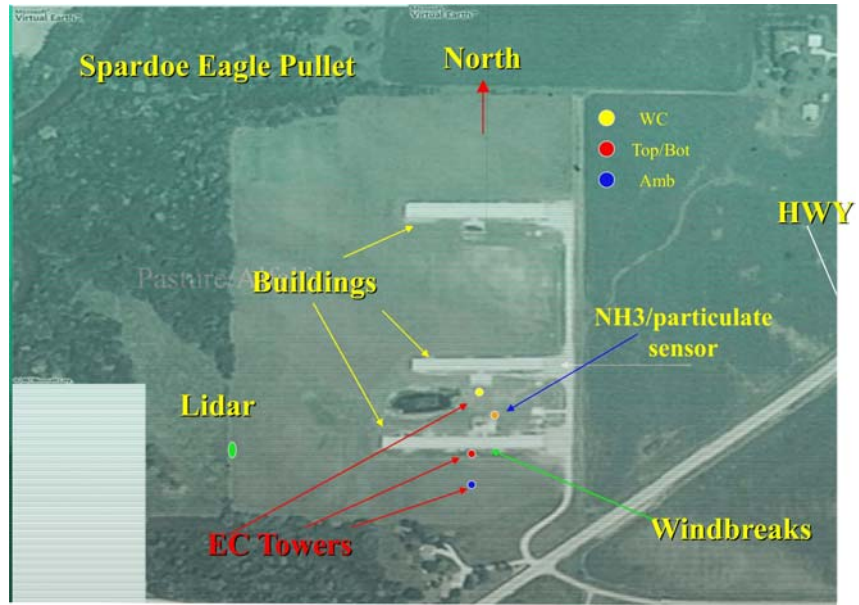


Figure 1. Overview of the Sparboe Pullet Facility near Eagle Grove, IA. and relative locations of the instrumentation for this study

as the turbulence

measurements to provide spatial and temporal images of particulate emissions from the south most building in response to building ventilation fan flow and wind flow modification in response to wind breaks and building structures.

III. INSTRUMENTATION DESCRIPTION

Elastic Lidar

Laser radars (lidars) are instruments that can map the three dimensional concentrations of certain components of the atmosphere. This allows the measurement and visualization of larger scale atmospheric flows. If the measurements can be taken fast enough, the evolution of the flow can be measured and visualized. Elastic lidars measure the backscattering from particulates. Raman lidars measure the absolute water vapor concentration.

The IIHR scanning miniature lidar (SMILI) seen in figure 2, is a small, scanning lidar that was designed to use elastic backscattering to determine the distribution and properties of atmospheric particulates. The lidar operates by emitting a pulse of infrared laser light into the atmosphere. Particulates interact with the pulse and scatter light back to the lidar. The term elastic refers to scattering in which no energy is lost by the photons, so that the detected light is at the same wavelength as the emitted light. The amount of returning light collected by the telescope is proportional to the cross sectional area of the water droplets in the air and the amount of atmospheric attenuation. The system is capable of both day and night operation.

A Nd:YAG laser operating at 1.064 (or 0.532) microns is the laser source. The laser is attached to 0.25 m, f/10, Cassegrain telescope. The laser beam is emitted parallel to the telescope after going through a periscope. The telescope-laser system is able to turn rapidly through 200 degrees horizontally and 100 degrees vertically using motors incorporated into the telescope mount. The system is entirely computer controlled through the use of various cards in the PC. This enables high speed data transfer and control of the scanning motors, which allows the capability to scan rapidly. The system can



Figure 2. A photograph of the miniature elastic lidar set up to map particulates in the field. This instrument took the data in figures 1 and 2.

be operated remotely and autonomously, using preprogrammed sequences which require an operator only to start.

Because the backscatter cross section for elastic scattering is large in comparison to most optical scattering processes, a small laser and telescope can be used and much faster time resolution is possible. The scanning system can be used to create vertical scans (also known as Range-Height Indicator or RHI scans) showing the relative particulate scattering within a vertical slice of the boundary layer. These can be done with a time resolution of less than 10 seconds. The small size of the lidar coupled with its fast scanning capability and sophisticated scanning and analysis methods make this lidar unusually capable and versatile.

The ability to measure particulates quickly is fortuitous in that particulates are a component of odor plumes and are closely related to odor from cattle, swine and poultry facilities. Many odorous compounds are easily absorbed onto and carried by particulates (Laird, 1997, SOTF, 1995). In a given volume of air, particulates may have absorbed many times the amount of some odorous compounds than is found in vapor form in the same volume of air. Particulates then concentrate some of the more obnoxious odors (OCTF, 1998). The importance of dust in the transportation of odor from livestock buildings has been well documented (OCTF, 1998; Thernilius, 1997; Laird, 1997; SOTF, 1995; Carpenter and Mouldsley, 1986; Hartung, 1986; Hammond et al., 1981; Hammond and Smith, 1981).

The lidar was located at the far edge of the field to the west (fig 1). There were only a few siting options for the system that were beyond the minimum sensitive range of the instrument (the lidar cannot “see” closer than about 125 m). This position allowed the system to

scan so that vertical slices of the atmosphere were oriented nearly perpendicular to the mean wind.

Ammonia Analyzer

The ammonia sensor is a rack-mounted, Pranalytica Nitrolux analyzer (fig 3) capable of measuring 4 incoming gas lines with a sensitivity of less than 1 ppb.

The instrument uses laser photoacoustic spectroscopy which involves absorption of radiation by specific NH₃ molecular absorption lines, followed by collisional de-excitation of NH₃ and simultaneous heating of the gas in the sample cell, and then detection of the acoustic energy generated

using a sensitive microphone. The Nitrolux system uses a carbon dioxide infrared gas laser, which is tuned to an absorption feature unique to NH₃. The wavelength (or frequency) is modulated on and off the absorption feature using a modulation frequency in the range 10-100 Hz. The use of an absorption line unique to ammonia makes the instrument immune from interference from routinely encountered industrial chemicals and other solvents that often confound conventional measurement techniques. Measurements are generated every 35 seconds although the response time is as much as two minutes for large step changes in concentration.

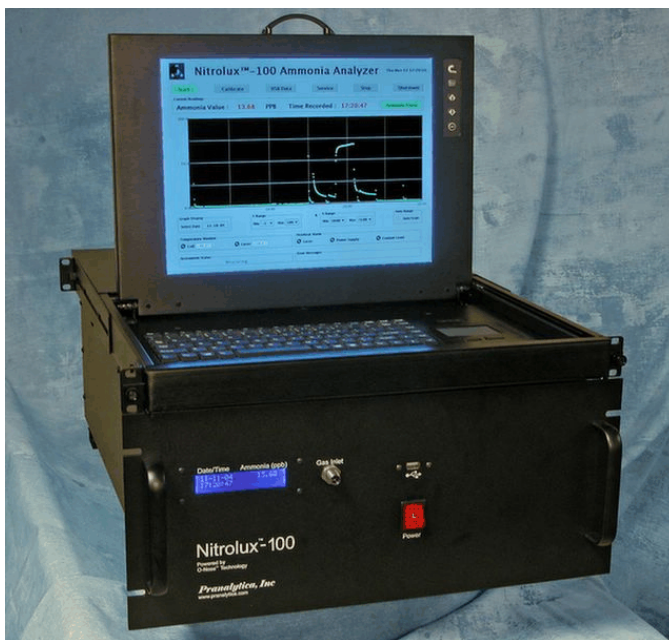


Figure 3. A photograph of the Nitrolux Ammonia analyzer. The system has a sensitivity of less than 1 ppb.

An internal vacuum pump continuously draws air into the device through a particulate filter on each line.

Particle Size Analyzer

The Particle size analyzer used in the campaign is an ELPI (Electrical Low Pressure Impactor) manufactured by Dekati (fig 4). The ELPI is capable of real time measurement of the particle size distribution and concentration in the size range of 30nm - 7 μ m. The ELPI combines impactor technology with particle charging and electrical detection. The ELPI operates by charging the particles to a known charge level in a unipolar corona charger. The particles are then size classified in a low pressure cascade impactor with



Figure 4. A photograph of the ELPI particle size analyzer.

electrically insulated collection stages according to their aerodynamic diameter. The accumulated charge in each stage is measured in real time by sensitive multi-channel electrometers. The measured currents are converted to an aerodynamic size distribution using particle size dependent relations describing the properties of the charger and the impactor stages. The result is particle number concentration and size distribution in real-time (measurements are made every 10 seconds). The components are housed in a single compact unit that is controlled by an external computer through a standard RS232 port.

The particle and ammonia analyzers were located approximately 25 m downwind of the first building (see fig 1). The exact siting was done so that the lidar had a clear line of sight and could scan within 3 meters of the location. This provided a calibration point for one pixel of the lidar scans (essentially a conversion factor to convert extinction coefficient, that the lidar measures, to an absolute particulate concentration (mg/m^3)). The value of the calibration of this pixel can be applied to all of the data in a scan to produce a two dimension plot of the absolute concentrations. The two instruments had their inlets 5 cm apart.

Meteorological Systems

The fundamental process responsible for the transport of any quantity (heat, water vapor, carbon dioxide, ammonia, particulates etc.) from a surface to the atmosphere adjacent to the surface (boundary-layer) is turbulence. Turbulence is different from the mean wind flow in that it represents deviations from the mean flow characteristics. Turbulence is three dimensional, rotational and chaotic in motion. It is the most efficient means of exchange of any property near the surface with the over lying atmosphere in contact with the surface. With respect to this study this would be the transport of particulates from a building into the surrounding boundary-layer of the atmosphere. Measuring turbulence

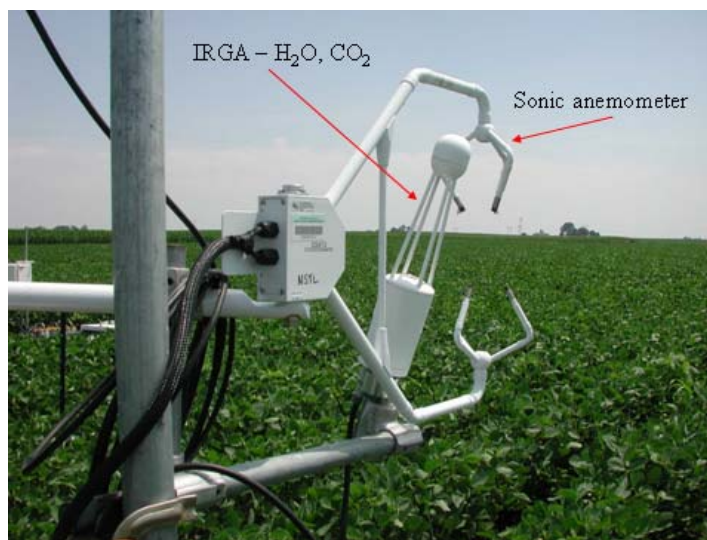


Figure 5. Close up of EC instrumentation. Sonic anemometer and Infra-red gas analyzer.

properties requires high frequency measurements of the three wind components (streamwise, lateral and vertical flows). This is accomplished with a 3-D acoustic (sonic) anemometer that measures wind velocity components (three directions) at a rate of 20 times per second or 20 Hz. In this study we used four sonic anemometers collocated with fast response Infra-red analyzers to



Figure 6. Space between south building and windbreak. Note the 10 m EC tower near the center of the image and the multiple banks of fans.

measure heat, water vapor, carbon dioxide and turbulence in the vicinity of the south poultry building. The collocation of a sonic anemometer with an IRGA is called eddy covariance (EC) and is an established meteorological technique to measure fluxes of energy and mass from a surface to the boundary-layer (fig 5). The first EC was located south of the wind break (Fig. 1) in an open area and represented the approach field to the buildings when the wind was originating from the south-southwest. The 2nd and 3rd EC systems were located on a 10 m (~33 ft) radio tower in between the south wall of the southern most building and the windbreak. This location represents a space that is influenced by the windbreak to the south, the bluff body of the building and the complex of exhaust fans on the south side of the building (fig 6). One EC was mounted ~2.5 m (~8 ft) above the ground and the other at ~ 8.5 m (28 ft) above the ground. The last EC system was mounted on a 5 m (16.4 ft) tower in the grass area between the southern most building and the next building north of it (Fig. 1). The data were collected continuously

throughout the study and stored on compact flash cards and ultimately on to laptops. The configuration of the EC towers was designed to maximize the general prevailing wind direction at that time of year for this location which was south to north. With the Lidar positioned ~140 m (~460 ft) due west and slightly south of the southern most building, when winds were southerly we were able measure particulate concentrations and turbulence characteristics in the approach region, the within building and windbreak region and the downwind space north of the south building. When winds were from the West, North or East these periods were not considered in the analysis.

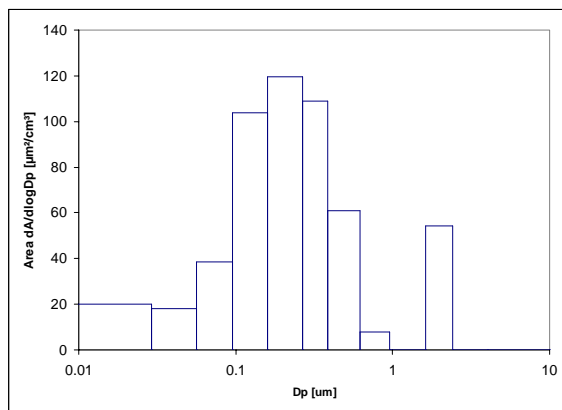


Figure 7. An example of the cross sectional size distribution from Aug 31. The lidar essentially measures the total of the cross sections of the particles in a given volume.

IV. RESULTS

Particle Size Analyzer

Data from the particle size analyzer allows one to measure the number and size of particles in time. This is convenient in that it allows examination of the data in a wide variety of ways. For

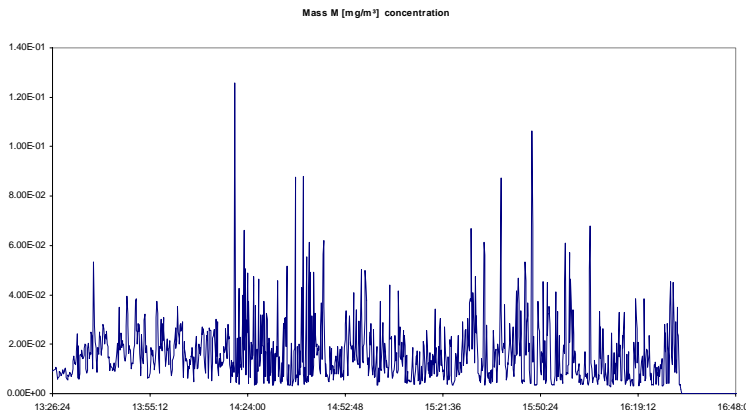


Figure 8. The mass concentration of particulates from 31 Aug. Note the “spiked” nature of the data indicating intermittent atmospheric motions with large concentrations.

example, the total volume (or mass) of the particles is of interest to regulatory agencies while for lidar purposes, we are interested in the total cross sectional area of the particles (which governs how much of the laser light is reflected). Obtaining a relationship between cross sectional area and total volume (or mass) of the particles enables us to convert a lidar scattering

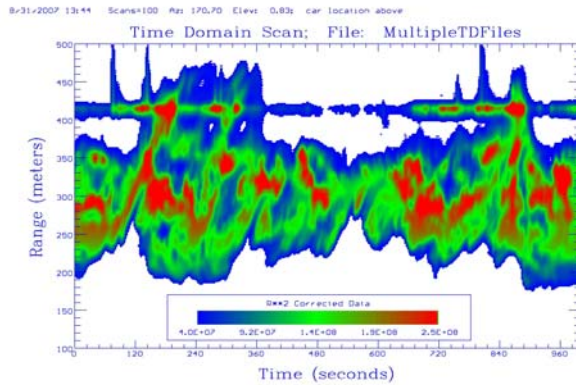


Figure 9. A plot of particulate concentrations derived from the lidar. This plot shows concentrations along a the length of the back of the first building (y axis) with time (x axis). Reds are highest concentrations blues are lower and white indicating ambient air.

measurement into a mass concentration measurement. Figure 7 is an example of a plot of the amount of cross sectional area as a function of particle size. Note that there are a large number of particulates in the 2 to 3 micron range. This is typical of agricultural operations. Note that in the mornings the average particulate

concentrations seem to decrease to a low level in the afternoon. This is an effect caused by relative humidity. At relative humidities above 85%, particulates will adsorb water and grow in size. In the

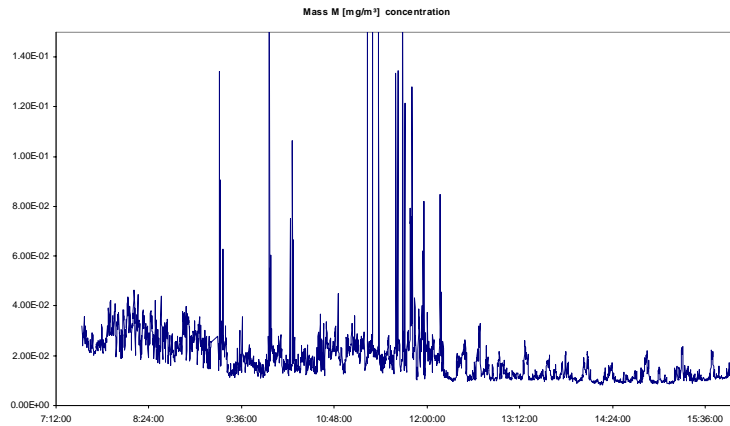


Figure 10. The particulate mass concentrations from Sept. 1st. While this data seems to be less “spiked” than that from the previous day (fig 8), it isn’t. This day does contain a limited number of events with extremely high concentrations.

afternoon, when it is much warmer, the relative humidity drops and this

does not occur. The period of the campaign was extremely wet, occurring just after the historic rains and flooding of August, 2007.

Figures 8 and 10 are examples of the mass concentrations in time. Of special note is the “spiked” nature of the data. This is indicative of an actively turbulent environment in which the mixing of clean ambient air and contaminated air from the buildings occurs. This is confirmed by the lidar data (fig 9) which also shows these parcels of air with elevated particulate concentrations. To make figure 9, the lidar was directed to look along the back of the first building, making measurements along that transect with time. As parcels of air with elevated concentrations move through the line of sight, they appear as red “blobs”. Figure 9 is typical of turbulent

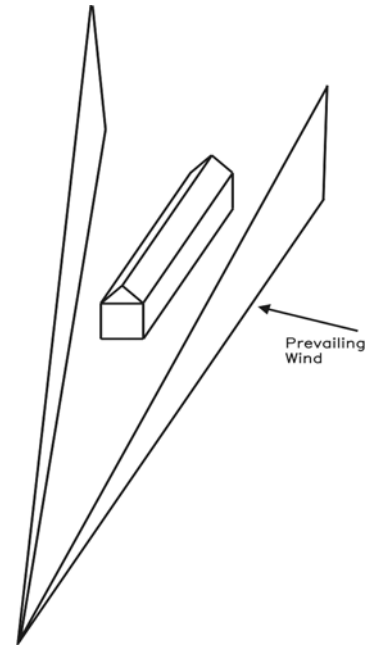


Figure 11. A plot of the lidar emission measurement concept. Measurement of the particulate concentrations upwind and downwind of the building enable estimation of the emissions from the building.

environments near sources. What is unusual is that the mixing is occurring at scales of tens of meters, far larger than expected. This is consistent with the meteorological data that shows an excess of atmospheric structures in that same size regime.

Elastic Lidar

The advantage of the elastic lidar is that it can make particulate concentration measurements over a large region. Thus it can provide images of

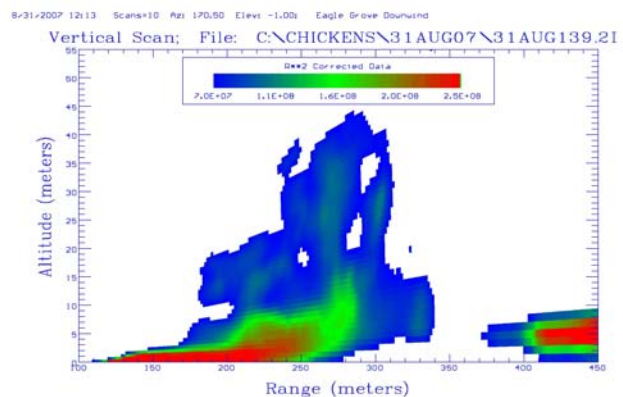


Figure 12. An example of a vertical slice of the atmosphere in the region between the building and windbreak. Red colors are high particulate concentrations, blues lower. White areas have ambient particulate loadings. The red area to the lower right is a north south windbreak on the far side of the building.

shapes of concentration levels in space. Judicious choice of scanning directions allows one to visualize sources and how the particulates move (indeed, the UI lidar can make successive scans fast enough to make “movies” of the emissions). The lidar was sited so that when it made a vertical scan (providing the

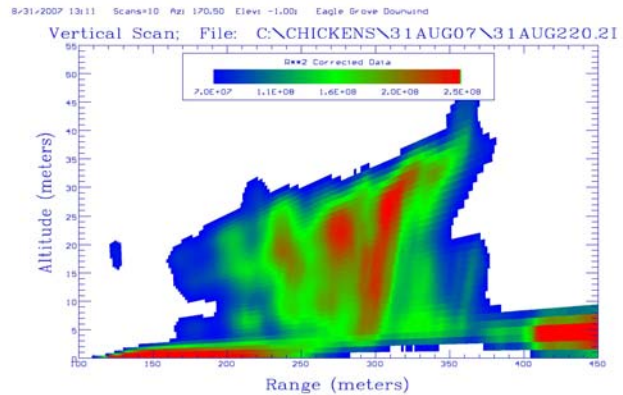


Figure 13. An example of a vertical slice of the atmosphere downwind of the first building. Three plumes are visible, one from each set of fans. Again note the amount of lofting that occurs, far above the height of the buildings.

concentrations in a vertical slice of the atmosphere), the scan was oriented nearly perpendicular to the mean wind. This was done so as to make a logical box around the first building. As shown in figure 11, by making a slice on both the upwind and downwind sides of the building, we can measure the amount of particulates that enters and leaves the volume of air surrounding the building (assuming that none leaves vertically). Slices were made upwind, next to the upwind meteorological tower and downwind near the particulate and ammonia sensors. To observe the air flow in the region between the building and the windbreak, another vertical slice was included between the meteorological tower and the windbreak. A set of measurements consisted of these three vertical sliced repeated every minute and a half.

Figure 12 is an example of a vertical slice of the atmosphere between the building and the windbreak. At a height of 15-20 m, one can identify three distinct plumes; one from each of the three sets of exhaust fans. At this particular time there was a small component of the wind from west to east (the major part was south to north). One can see that the wind channeled the particulates to the east (towards the right of the figure). Note also the lofting of the particulates

high above the building (> 40 m). Lofting this high is not a part of conventional emissions modeling of these kinds of facilities. Conventional downwind emissions modeling assumes a conventional Gaussian plume model in which the emissions are at or near the surface. The lidar images clearly show lofting high above the buildings. The good news is that this lofting greatly reduces low level concentrations and thus the risk to persons at the surface. However, emission factors based on near surface concentration measurements are probably subject to considerable error.

Figure 14 has an example of an upwind concentration profile and a downwind one as well. The scale of the upwind profile has been changed so that the differences in ambient concentration can be seen. Very small (~3 %) changes in ambient concentrations can be detected by the instrument. The slightly redder area near 400 m is the result of the passage of a diesel truck. The intense red area at the bottom is the shape of the land surface. The downwind profile here has been inverted to obtain spatially resolved mass concentrations. The sum of the product of the mass concentrations at each height by the wind speed at that height and by the

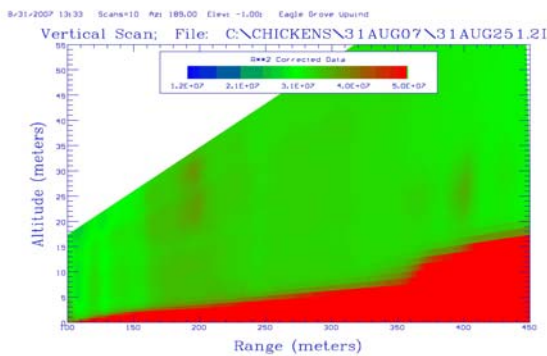


Figure 14a. An example of an upwind vertical slice. The scale is changed here so that the natural variations in ambient particulate concentration can be seen. The slightly higher concentration at 400 m is from the passage of a diesel truck. The intense red at the bottom is the shape of the land surface.

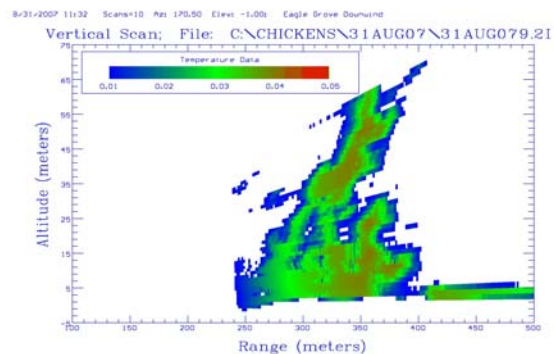


Figure 14b. An example of a downwind vertical slice that has been inverted to obtain spatially resolved particulate mass concentrations. This plot, when combined with a wind profile will allow estimation of the particulate emission rate.

area represented by the measurement is the flux of particulates through that plane (milligrams of particulates per second). When the particulate flux from upwind is subtracted from this value (usually a number of order 0.5% of the downwind value), this value of the particulate emission rate from the building is obtained. We believe this method is the most effective answer to the NRC challenge of a method to estimate total downwind emissions. The method may be applied to any substance that is measurable by lidar.

Ammonia Analyzer

The ammonia analyzer, located with the particulate analyzer shows essentially the same phenomenology as the particulate analyzer. The data shows intermittent high concentration

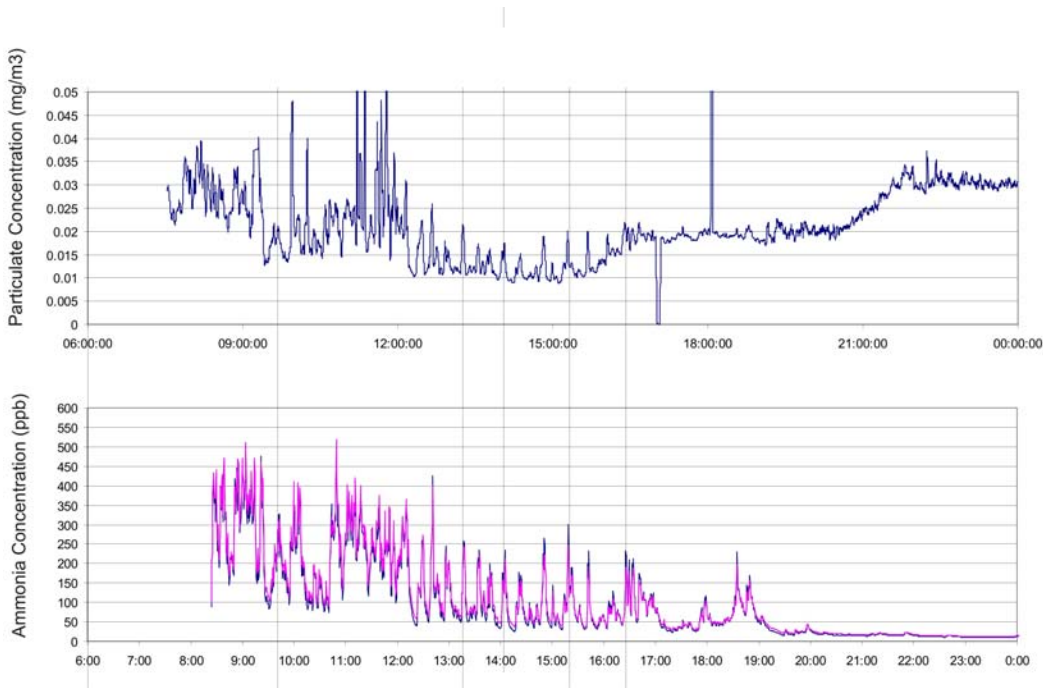


Figure 15. A comparison of the particulate and ammonia concentrations for Sep 1st. Note that both instruments show intermittent high concentrations at the same time. Four vertical lines are drawn to show the same times in each graph.

spikes that occur on semi-regular periods. The ammonia sensor has a much longer response time to changes in concentration, so that it does not have the detail that the particulate data does. The peaks in the ammonia data are broader and not as pronounced. This is a characteristic of the ability of the sensor to measure sharp changes in time. That the two sensors show spikes at the same time confirms that air masses of order 10-20 m in size containing high concentrations of particulates and ammonia (from the facility) are being mixed with the ambient air. It also shows that high ammonia concentrations are found in air masses with high concentrations of particulates. The relative levels of each are not constant so that a particulate level of some given value does not imply any particular ammonia level. However, it does indicate that the ammonia and the particulates are emitted together and are transported in the same way. In turn this is important in that it demonstrates that particulates are a good tracer for how the emissions are transported. So that for example, the lidar images that show particulates are lofted high above the buildings imply that ammonia is lofted as well. Tracking the particulates turns out to be much simpler than tracking ammonia.

Meteorological Systems

Data from the four EC systems were selected to meet what was considered the ideal conditions for this study, namely southerly wind flow. In this case wind approaching the building complex from the south would first cross an open alfalfa field directly south of the south most building. Lidar scans or observations in this approach area would be considered ambient conditions (clean air); that is air that has not been contaminated by particulates from a confined animal source. Eddy covariance measurements from the tower in the ambient location would

represent wind flow and turbulence characteristics in an “undisturbed” flow that is to say mean flow and turbulence properties that were in equilibrium with the upwind surface (in this case a low smooth alfalfa field) and not modified by obstacles such as wind breaks and buildings.

As the wind moves from the ambient position toward the wind break and the building, (channel region) the second EC tower is recording properties of the wind flow/turbulence properties that have been modified by the wind break, the building and the exhaust fans on the south side of the building. In the channel region there were two EC systems one at 2.13 m (~7 ft) designated as “bottom” (bot) the other at 8.22 m (~ 27 ft) AGL designated as “top”. The vertical distribution of the two EC systems (~ 2 and 8 m) in the channel region allow for the measurement and characterization of the mean flow and turbulence properties after significant modification from the shearing effect of the top of the windbreak (~6 m), low velocity air movement from the exhaust fan banks and the bluff body effect from the building itself. The final EC system designated as “within complex” (WC) was located at 5.57 m (~ 18 ft) AGL between the south building and the building just north of it. This tower represents a recovery position for the mean flow of the wind after undergoing modification from the encounter with the windbreak and south building. All of the EC measurements were continuous and made in conjunction with sequential vertical Lidar scans of particulate concentrations in the approach, channel and recovery regions. Example results from EC measurements are shown in Fig. 16. Here a panel of three plots of 30 minute average values of wind direction, mean wind speed (u) and friction velocity (u^*) for each of the four EC towers for September 01, 2007 between 1200 and 1600 hours. The wind direction is in general the same for the amb, top and wc locations with a minor difference for the amb position. The bottom (bot) is considerably having essentially

a northern component with respect to the other southerly directions. This is reasonable since at bot position the sonic is strongly under the influence of the exhaust fans. What is significant is the implication of a mechanically induced wind direction in a narrow channel that is counter to the mean wind direction of the atmosphere. The implication is the potential for the development of a micro vortex within channel that may contribute to the vertical lofting of particulates emitted by the exhaust fans. More information is needed to confirm this hypothesis however current results strongly suggest a micro vortex mechanism. In the mean wind panel, again we can observe a similar pattern to that of the wind direction. Increases and decreases in the mean wind speed appear to be rather coherent across the landscape with some differences in magnitude changes indicating the effects of the wind break, building obstacle and the smooth recovery grass surface. In the final panel showing friction velocity there appears some interesting and as yet unexplained pattern with respect to the amb location. It needs to be clarified at this point that the friction velocity can be considered as a suitable indicator of the turbulence intensity, the primary mode of transport from a surface to the atmosphere. The significantly larger friction velocity values in the amb position suggest increased turbulence intensity at this location possibly resulting from the southerly wind that interacts with the wind break. Part of the flow is lifted up over the top, part may permeate the wind break and still another may “roll” back onto the mean southerly flow that then enhances the friction velocity at the amb location. Put another way the amb EC tower may have been too close to the wind break.

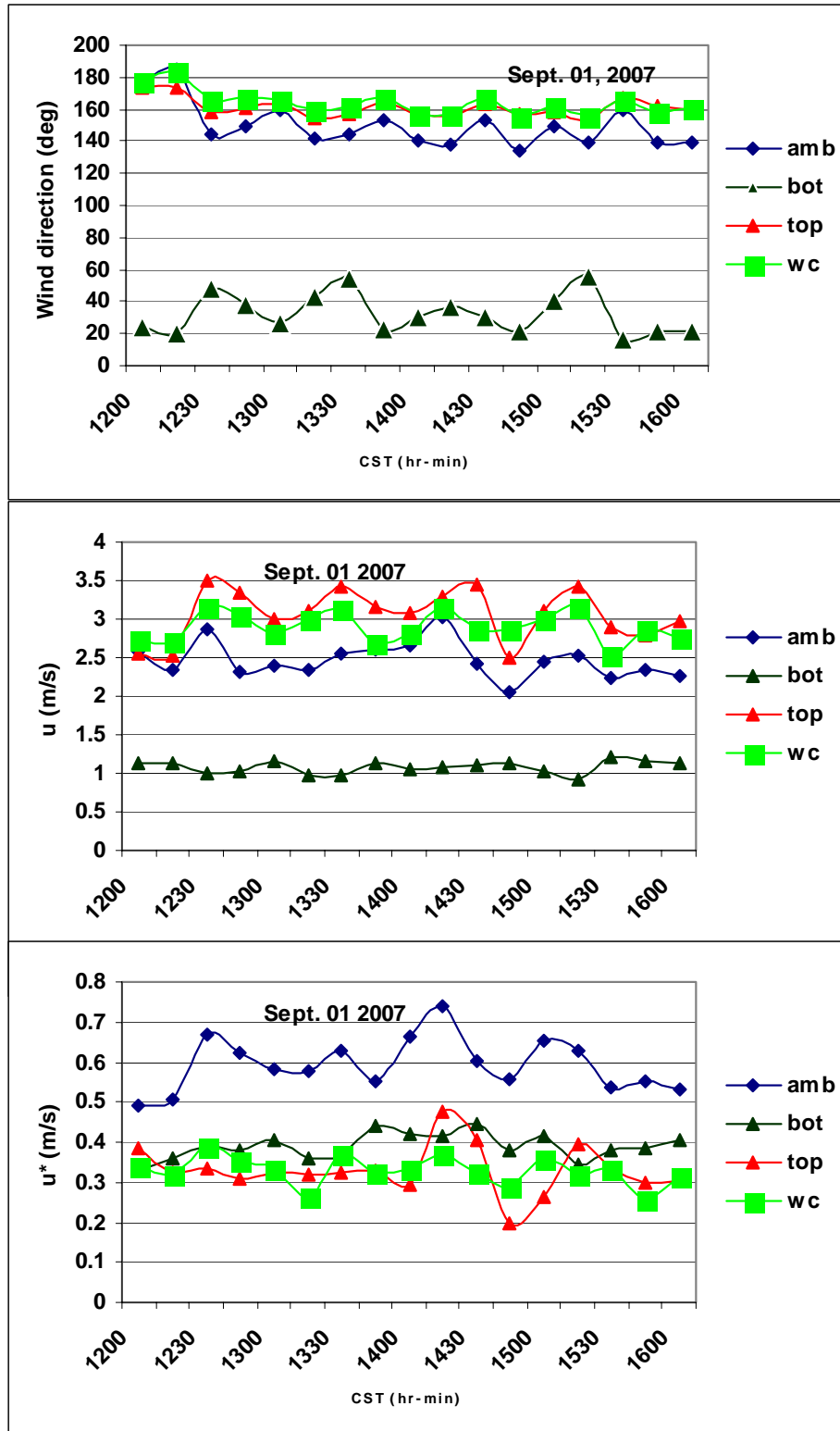


Figure 17. Variation in wind direction, speed and friction velocity for the four EC systems as a function of position in the landscape.

V. SUMMARY

The eddy covariance technique was initially developed to evaluate heat and water vapor exchange processes for flat uniform agricultural surfaces. As our understanding of turbulence exchange processes increased for these relatively simple applications (short flat agricultural surfaces) the need for understanding exchange processes for much more complex landscape scenarios involving animal facilities became a logical advancement to characterize emission loadings to the atmosphere of particulates and other trace gases such as ammonia. In this study we integrated the science of remote sensing with a Lidar with the science of turbulence measurements of the flow field surrounding a poultry facility to estimate emission loadings of particulates to the atmosphere. An additional component involved measuring ammonia loading as well with the intent to provide a sound scientific approach to evaluate fluxes of ammonia and particulate from a poultry facility based on a whole facility integration using the power of Lidar detection. Eddy covariance

measurements provide valuable information for turbulence transport properties. This information can be integrated with Lidar measurements of particulate concentrations to yield measurable and reliable whole facility estimates of particulate emissions from animal facilities. What was found in

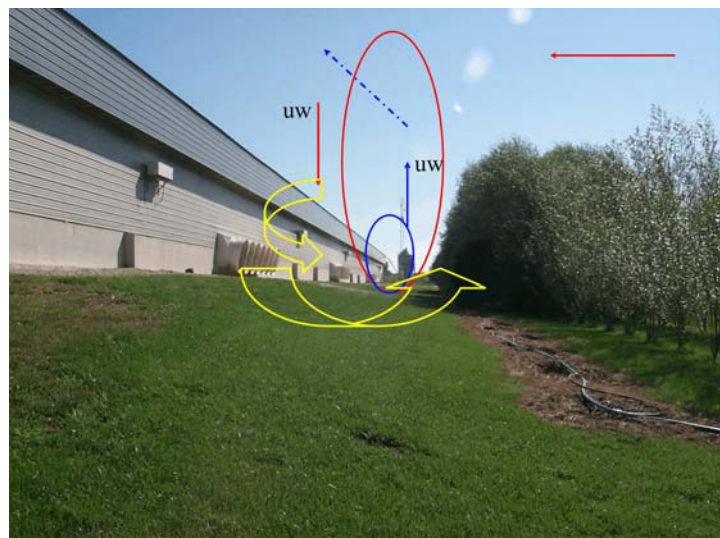


Figure 17. Depiction of the complex flow patterns developed within the channel region. uw indicates momentum or mass airflow.

this study showed the complex nature of plume emission as it was emitted from the exhaust fans into a micro-vortex generated in the channel region as a result of the interaction of the mean wind flow (from the south in this particular case) the windbreak and the building itself (Fig. 17). These micro-vortices have the potential to loft particulates and gases up into the boundary-layer. More information is needed to develop a model to predict such mechanical uplifts for a range of wind direction, speeds and surface stability conditions.

This study has provided an incredibly rich data set that will be examined for many years. Already it has enabled us to establish the following:

- * While shelter belts do a good job of filtering large items from the air (particularly parts of feathers as from this facility) and providing a visual shield of the site, it plays little role in the dispersal or lofting of effluents from these kinds of sites. The lofting that we observe occurs regardless of the presence or absence of the shelter belt.

- * Effluents from these facilities are lofted to altitudes roughly three times the height of the buildings. This seems to occur under nearly all types of unstable atmospheric conditions.

- * Ammonia and particulates, and by implication all of the effluents from the facility, travel together in the same atmospheric structures. This is important in that it allows us to track the motions of the particulate plumes (which can be done via lidar quite simply) and infer the motion and dilution of the effluents from observations of these effects on particulates. Ammonia and other trace gas sensors are expensive and cannot be deployed in the numbers needed to track the transport of these pollutants.

- * The transport and dispersion of the effluents near the facility appears to be governed primarily by atmospheric motions on a scale of 10 to 20 meters. These motions were first

identified on the power spectra of both the fluxes of materials, and in the wind components. The effects of these structures can be seen in both the particulate and ammonia concentrations (CO₂ and water vapor as well). These structures can also be seen in the lidar scans. Work remains to identify the source of these motions.

motions

VI. ACKNOWLEDGEMENTS

The team from the Soil Tilth Laboratory and the University of Iowa are grateful for the support of the Egg Council in making this happen. We also wish to acknowledge the assistance of the owner of the facility, , whose help was critical in coping with the rains and gaining access to the site.

VII. BIBLIOGRAPHY

Carpenter, G.A. and L.J. Mousley. 1986. Dust concentrations in pig buildings. pp.333-335. In:

Odour Prevention and Control of Organic Sludge and Livestock farming. Elsevier

Applied Science Publishers, New York, NY.

Cooper, D.E., and W.E. Eichinger, L. Hippias, J. Kao, J. Reisner, S. Smith, S.M. Schaeffer, and

D.G. Williams, (2000), Spatial and temporal properties of water vapor and flux over a riparian canopy. *Agric. And Forest Meteorol.* Special Issue, 105, pp 161-183,

Cunnick, J.E. 1995. Implications of environmental odor on psychological status and health.

International Livestock Odor Conference, October 16-17, 1995, Iowa State university.

Donham, K. 1998. Occupational Health Risks For Swine Producers: Inferences for Public Health

- Risks for People Living in the Vicinity of Swine Production Units, Manure Management Conference, Iowa State University 1998.
- Donham, K. 1998. The impact of industrial swine production on human health. pp.73-83. In: Thu, K.M. and E.P. Durrenberger, editors. 1998. Pigs, Profits, and Rural Communities. New York: State University of New York Press.
- Hammond, E. G., C. Fedler, and R.J. Smith. 1981, Analysis of particle borne swine house odors. *Agriculture and Environment*, **6**, 395-401.
- Hammond, E. G. and R. J. Smith. 1981. Survey of some molecularly dispersed odorous constituents in Swine house air, *Iowa State Journal of Research*, **55**(4):393-399.
- Hartung, J. 1985. Dust in livestock buildings as a carrier of odours. pp.321-332. In: *Odour Prevention and Control of Organic Sludge and Livestock farming*. Elsevier Applied Science Publishers, New York.
- Hatfield, J.L., Prueger, J.H., Cionco, R.M., Sauer, T.J., Pfeiffer, R.L., Hipps, L.E., and Zahn, J.A., 2000, Air flow and microclimate around earthen manure storage units. Proc. Air Pollution from Agricultural Operations. ASAE., St. Joseph, MI. pp. 124-131..
- Homes, M. J., A. J. Heber, C. C. Wu, L. K. Clark, R. H. Grant, N. J. Zimmerman, M. A. Hill, B. R. Strobel, M. W. Peugh, and D. D. Jones. 1995. Viability of Bioaerosols produced from a swine facility. <http://www.anr.ces.purdue.edu/anr/anr/swine/house/conf.htm>
- Holmén, B.A., W.E. Eichinger, and R.G. Flocchini, “Application of Elastic Lidar to PM₁₀ Emissions from Agricultural Nonpoint Sources”, *Environ. Sci. Technol.* **32**, 3068 – 3076 (1998).

- Laird, D.J. 1997. Wind tunnel testing of shelterbelt effects on dust emissions from swine production facilities. Thesis (M.S.)--Iowa State University.
- National Research Council. 2003. Air Emissions from Animal Feeding Operations: Current Knowledge, Future Needs. National Academies Press, Washington, DC. 263 p.
- Odor Control Task Force (OCTF). 1998. Board of Governors of the University of North Carolina. Control of odor emissions from animal Operations.
- Schiffman, Susan S. et al., 1995, The Effect of Environmental Odors Emanating From Commercial Swine Operations on the Mood of Nearby Residents, *Brain Research Bulletin*. **37**, 4: 369-375.
- Swine Odor Task Force (SOTF). 1995. Options for Managing Odor. North Carolina University, <http://www.ces.ncsu.edu/whpaper/SwineOdor.html>
- Thernelius, S.M. 1997. Wind tunnel testing of odor transportation from swine production facilities. Thesis (M.S.)--Iowa State University, 1997